

# Detection via simultaneous trajectory estimation and long time integration

Kimin Kim, *Student Member, IEEE*, Murat Üney, *Member, IEEE*, and Bernard Mulgrew, *Fellow, IEEE*

**Abstract**—In this work, we consider the detection of manoeuvring small objects with radars. Such objects induce low signal to noise ratio (SNR) reflections in the received signal. We consider both co-located and separated transmitter/receiver pairs, i.e., mono-static and bi-static configurations, respectively, as well as multi-static settings involving both types. We propose a detection approach which is capable of coherently integrating these reflections within a coherent processing interval (CPI) in all these configurations and continuing integration for an arbitrarily long time across consecutive CPIs. We estimate the complex value of the reflection coefficients for integration while simultaneously estimating the object trajectory. Compounded with this is the estimation of the unknown time reference shift of the separated transmitters necessary for coherent processing. Detection is made by using the resulting integration value in a Neyman-Pearson test against a constant false alarm rate threshold. We demonstrate the efficacy of our approach in a simulation example with a very low SNR object which cannot be detected with conventional techniques.

**Index Terms**—radar detection, coherent integration, non-coherent integration, bi-static radar, multi-static radar, target tracking, synchronisation.

## I. INTRODUCTION

THE detection of manoeuvring and small objects with radars is a challenging task [1] and is a highly desirable capability in surveillance applications [2]. Radars emit modulated pulses towards a surveillance region and collect reflected versions of the transmitted waveforms from objects in this area. Small objects induce low signal-to-noise ratio (SNR) signals at the radar receiver. The decision on object presence is made by testing the hypothesis that the received signal contains reflections against the noise only signal hypothesis after the front-end input is filtered with a system response matching the probing waveform, which is known as the matched filter (MF) [3].

In order to detect low SNR objects, many such pulse returns (i.e., multiple measurements) need to be considered as each reflection is at a level similar to the noise background. The sufficient statistics of multiple pulse returns are found by summing the associated reflection coefficients across them, which is referred to as pulse integration [3, Chp.8]. This process is applied on the sampled outputs of the MF stage. These samples correspond to, in effect, measurements corresponding to resolution bins in an equally divided range space. In

This work was supported by the Engineering and Physical Sciences Research Council (EPSRC) grant EP/K014277/1, and, the MOD University Defence Research Collaboration (UDRC) in Signal processing.

K. Kim, M. Üney, and B. Mulgrew are with Institute for Digital Communications, School of Engineering, the University of Edinburgh, Edinburgh, EH9 3JL, U.K. (e-mail:{K.Kim, M.Uney, B.Mulgrew}@ed.ac.uk).

conventional processing, beamforming and doppler processing with these samples are used to further segment the bearing and Doppler space into resolution bins and find the corresponding measurements. Conventional methods for integration over time such as coherent and non-coherent integration integrate pulse returns in the same range-bearing and Doppler bins across time. When objects manoeuvre, however, these reflections follow a trajectory across these bins, and, these methods fail to collect evidence on object existence for a long time due to not taking into account this trajectory. On the other hand, longer integration time provides higher probability of detection for a given false alarm rate, in principle.

One possible solution to providing long time integration for manoeuvring objects is to design filters with long impulse responses that match multiple pulse returns along a selection of possible trajectories (see, e.g., [4]& [5]). The number of filters required in this approach easily becomes impractically excessive with increasing integration time. An alternative approach is to employ a dynamic programming perspective and use a regular probing pulse MF to integrate its outputs along a trajectory estimated simultaneously which corresponds, in a sense, to online adaptive synthesis of long time MFs.

Trajectory estimation using the outputs of a pulse MF is often referred to as track-before-detect (see, for example, [6], [7]). The sample that corresponds to the true object kinematic state (i.e., location and velocity) is a complex value that is a sum of the reflection coefficient and background noise [8]. Most track-before-detect algorithms, on the other hand, use the modulus of the MF within models which describe the statistics of the modulus of the MF output. These models are averaged and hence cannot fully exploit the information captured by the measurements. For example, it is well known that the detection performance of these methods can be improved by also taking into account the phase of the data samples [9], in addition to the modulus.

The best achievable detection performance is obtained by coherent processing [3], in which one needs to estimate the complex reflection coefficient from the complex values of the MF outputs, the latter of which are processed by the aforementioned algorithms. This corresponds to using a non-averaged model in which the reflection coefficient is a random variable that remains the same during what is known as a coherent processing interval (CPI), and, is generated randomly for consecutive CPIs [8]. This is challenging partly because estimation of this quantity with a reasonable accuracy requires more samples than one can collect at the pulse-width sampling rate in a coherent processing interval (CPI) [10]. For example, in [11], coherent processing and integration within a CPI is

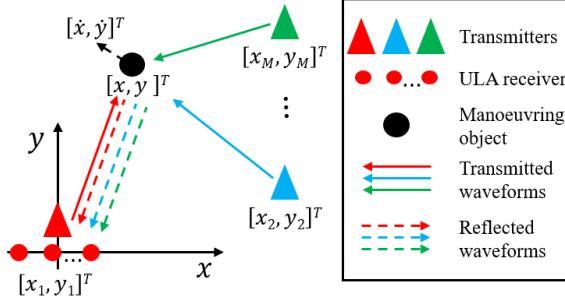


Fig. 1. Problem scenario:  $M$  transmitters and a ULA receiver to detect a small object located at  $[x, y]^T$  with velocity  $[\dot{x}, \dot{y}]^T$ .

performed with a very high sampling rate that yields a large number of samples in the pulse interval.

In [12], we demonstrated that this can be remedied using a phased array receiver structure. In particular, we introduced a simultaneous trajectory estimation and long time integration algorithm in which the integrated value is then tested against a constant false alarm rate (CFAR) threshold for declaring the existence or otherwise of an object in a Neyman-Pearson sense. In [13], we extend this approach for separated transmitter/receiver pairs, i.e., bi-static channels, with an unknown time reference shift. We recover the synchronisation term by diverting simultaneous beams towards the tested point of detection and the remote transmitter thereby relaxing the commonly used assumption that the remote transmitters and the local receiver are synchronised (see, e.g., [14], [15]).

In this work, we provide a complete exposition of our long time integration and trajectory estimation approach in mono-static and bi-static configurations as well as the multi-static case. In particular, we consider the system structure in Fig. 1 where there are multiple transmitters using mutually orthogonal waveforms. The receiver is a ULA and has the full knowledge of the transmission characteristics except the time reference shift of the separately located transmitters. The front-end signals at the receive elements are the superposition of noise, signals from direct channels, and, reflections from objects.

We consider a long time likelihood ratio test conditioned on a trajectory in a kinematic state space, reflection coefficients, and, synchronisation terms as unknown parameters. In order to estimate the kinematic quantities, we use a Markov state-space model in which the object state consists of location and velocity variables. The measurement model of this state space model involves the radar ambiguity function parameterised on the aforementioned reflection coefficients. These coefficients are estimated by using an expectation-maximisation algorithm [16] realising a maximum likelihood (ML) approach within Bayesian filtering recursions for state trajectory estimate. We show that this is an empirical Bayesian method [17] for realising the update stage of the filter. Then, we prove that the Cramér-Rao lower bound (CRLB) for this estimate is inversely proportional with the number of array elements, and, hence a very accurate estimate can be obtained using a sufficiently large aperture even for short CPIs. Owing to this accuracy, the empirical Bayes update is an accurate

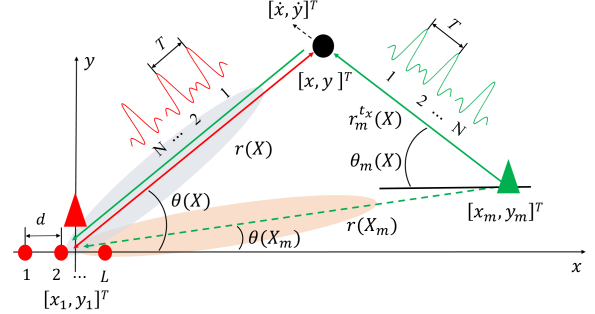


Fig. 2. Geometry of the problem: A ULA receiver co-located with a transmitter and another transmitter placed in a separate location on the 2D Cartesian plane. Both polar and Cartesian coordinate variables are depicted. Each transmitter emits  $N$  pulses in a CPI. The waveforms used are orthogonal.

approximation to the otherwise intractable filtering update equations. For synchronisation, we employ a digital beam-forming technique to simultaneously divert beams towards both the test points of detection and the locations of the separately located transmitters in order to find the respective time reference shifts in the bi-static channels.

The resulting algorithm enables us to collect the entire evidence of object existence at the receiver by i) performing coherent integration in both mono-static and bi-static channels within a CPI, ii) non-coherently integrating across different (non-coherent) channels, e.g., local mono-static and remote bi-static channels, and, iii) continuing integration for an arbitrarily long interval that contains many CPIs. As a result, this approach enables us to detect manoeuvring and low SNR objects which cannot be detected using other techniques.

This article is organised as follows: Section II gives details of the problem scenario and introduces the mathematical statement of the problem. In Section III, we discuss trajectory estimation with the array measurements and detail the aforementioned empirical Bayes approach. Then, we introduce the ML estimator using an expectation-maximisation algorithm for the complex reflection coefficients and the CRLB. We also detail the synchronisation approach in Section IV. We combine these estimators and specify the proposed detection scheme in Section V. The proposed detection algorithm is demonstrated in Section VI through an example scenario in which a manoeuvring very low SNR object is to be detected. Finally, we conclude in Section VII.

## II. PROBLEM STATEMENT

Let us consider the problem scenario in Fig. 1 with a ULA receiver (depicted by red dots), and,  $M$  transmitters (depicted by triangles) one of which is co-located with the receiver forming a mono-static pair. The other transmitters are located elsewhere and form bi-static pairs with the receiver.

The receiver is comprised of  $L$  elements spaced with a distance of  $d$  which will be specified later in this section. Each element collects reflected versions of the transmitted waveforms emitted by both the co-located and the separately located transmitters thereby forming mono-static and bi-static pairs, respectively.

### A. Spatio-temporal signal model

A detailed model for the signals induced at the receiver array by reflections from an object is as follows: We consider an interval of time in which each transmitter emits  $N$  consecutive waveforms  $\tilde{u}_m(t)$  separated by a time length of  $T$  after modulating with a common carrier that has an angular frequency of  $\omega_c = 2\pi f_c$ . The  $m$ th transmitted signal is therefore given by

$$u_m(t) = \operatorname{Re} \left\{ \sum_{n=0}^{N-1} \tilde{u}_m(t - nT) e^{j\omega_c t} \right\}, \quad (1)$$

where  $\operatorname{Re}\{\cdot\}$  denotes the real part of its input complex argument and  $T$  is known as the pulse repetition interval (PRI).

We assume that  $\{\tilde{u}_m\}_{m=1}^M$  is an orthogonal set of waveforms of pulse duration  $T_p$  and bandwidth  $B$ , i.e.,

$$\begin{aligned} \langle \tilde{u}_m(t), \tilde{u}_{m'}(t) \rangle &\triangleq \int_0^{T_p} \tilde{u}_m(t) \tilde{u}_{m'}^*(t) dt \\ &= \delta_{m,m'} \end{aligned} \quad (2)$$

for  $m, m' \in \{1, \dots, M\}$ , where  $\delta_{m,m'}$  is Kronecker's delta function.

Use of such orthogonal transmit waveforms underlies the vision of multiple-input multiple-output (MIMO) radars [18], [19] a particular configuration of which is, hence, the system considered here. Design of orthogonal sets for MIMO sensing was investigated with various objectives such as maximisation of diversity [20] and waveform identifiability [21]. In this work, we consider a narrowband regime in which frequency division multiplexing can be used to achieve orthogonality in practice.

In order to specify the received signal at the array elements, let us consider the geometry of the problem which is illustrated in Fig. 2 for  $M = 2$  transmitters. The receiver array measures the superposition of signals from different channels which are depicted by coloured lines. In particular, there are i) a local (mono-static) channel (red line), ii) a remote (bi-static) channel (green line), and, iii) a direct channel from the remote transmitter (green dashed line). The first two are reflection channels propagating the reflected waveforms from the object (black circle) towards the receiver array. These channels can be fully separated given the array data by exploiting the orthogonality of the waveforms over time and the capability of spatial filtering thereby diverting multiple beams towards arbitrary arrival angles, simultaneously. These points will become clear in the sequel.

Let us model the signals in the reflection channels. We assume that the reflectivity of the object remains coherent (i.e., unchanged) during the collection of reflections from the  $N$  pulses in (1). Such a time interval is known as a coherent processing interval (CPI). Modelling of the direct channel signals is introduced later in Section IV-B.

The kinematic state of the reflector (depicted by a black dot) in the 2D Cartesian plane is given by  $X = [x, y, \dot{x}, \dot{y}]^T$ , where  $[x, y]^T$  is the location,  $[\dot{x}, \dot{y}]^T$  is the velocity, and  $T$  denotes vector transpose. The distance of  $X$  to the receiver is related to pulse time of flights. The overall distance a pulse emitted by the  $m$ th transmitter at  $[x_m, y_m]^T$  and reaches the receiver

at  $[x_1, y_1]^T$  after getting reflected at  $[x, y]^T$  is given by

$$\begin{aligned} R_m(X) &= R_m^{tx}(X) + R(X) \\ R_m^{tx}(X) &\triangleq \sqrt{(x - x_m)^2 + (y - y_m)^2} \\ R(X) &\triangleq \sqrt{(x - x_1)^2 + (y - y_1)^2} \end{aligned} \quad (3)$$

where  $R_m$  and  $R$  denote the distance from the object to the  $m$ th transmitter and to the receiver, respectively.

The corresponding time of flights are found as

$$\begin{aligned} \tau_m(X) &= \tau_m^{tx}(X) + \tau(X) \\ \tau_m^{tx}(X) &\triangleq \frac{R_m^{tx}(X)}{c}, \quad \tau(X) \triangleq \frac{R(X)}{c}, \end{aligned} \quad (4)$$

where  $c \approx 3.0 \times 10^8 \text{ m/s}$  is the speed of light.

The velocity of the object induces an angular frequency shift on reflections which is known as the Doppler shift. This quantity is given by

$$\Omega_m(X) = \frac{2\pi T}{\lambda_c} \left( \dot{x} \times (\cos \theta(X) + \cos \theta_m(X)) \right. \\ \left. + \dot{y} \times (\sin \theta(X) + \sin \theta_m(X)) \right), \quad (5)$$

where  $\theta$  and  $\theta_m$  are the angle of arrival (AoA) of the reflections to the receiver and the bearing angle of the object with respect to the  $m$ th transmitter, respectively. These quantities are given by

$$\begin{aligned} \theta(X) &= \arctan(y_1 - y)/(x_1 - x) \\ \theta_m(X) &= \arctan(y_m - y)/(x_m - x). \end{aligned} \quad (6)$$

For narrowband reflections, the signals induced at the array elements are characterised by a spatial steering vector as a function of  $\theta$  which is given by [22, Chp.2]

$$\mathbf{s}_s(\theta) = \left[ 1, e^{-j\omega_c \frac{d}{c} \sin \theta}, \dots, e^{-j\omega_c (L-1) \frac{d}{c} \sin \theta} \right]^T,$$

where  $d$  is the separation between the array elements selected as half of the carrier wavelength, i.e.,  $d = \lambda_c/2$ . Substituting this quantity together with  $c = \lambda_c \times f_c$  in the equation above leads to

$$\mathbf{s}_s(\theta) = \left[ 1, e^{-j\pi \sin \theta}, \dots, e^{-j(L-1)\pi \sin \theta} \right]^T. \quad (7)$$

The superposition of the reflections after demodulation at the receiver is given using (7) and (5) by

$$\begin{aligned} \mathbf{z}(t) &= \mathbf{s}_s(\theta) \sum_{m=0}^{M-1} \sum_{n=0}^{N-1} \alpha_m e^{jn\Omega_m} e^{-j\omega_c (\tau_m + \Delta t_m)} \\ &\quad \times \tilde{u}_m(t - \tau_m - \Delta t_m - nT), \end{aligned} \quad (8)$$

where  $\alpha_m$  is a complex coefficient modelling the reflectivity in the  $m$ th channel, and,  $\tau_m$  is the time of flight of a pulse given in (4). Here,  $\Delta t_m$  is an unknown time shift modelling the time reference difference between the  $m$ th transmitter and the receiver (i.e., a synchronisation term).

The reflections in the received signal are optimally searched by matched filtering [8], i.e., by convolving the input with inverted versions of the probing waveforms. In our scenario, this corresponds to a bank of  $M$  filters, (see, e.g. [19, Chp.3]). Owing to the orthogonality (asserted by (2)), the  $M$  channels

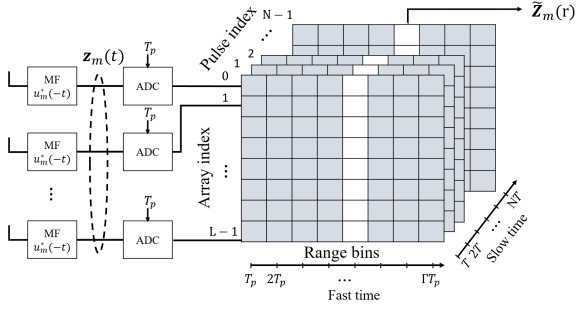


Fig. 3. Data acquisition in the  $m$ th channel: Sampled version of the received signal within a CPI as a radar data cube. The output of the matched filter is sampled and arranged in array index, fast time and slow time axis.

in (8) will have been separated at the filter outputs<sup>1</sup>. The output of the  $m$ th filter is given by

$$\begin{aligned} \mathbf{z}_m(t) &\triangleq \mathbf{z}(t) * \tilde{u}_m(-t) \\ &= \alpha_m \mathbf{s}_s(\theta) \sum_{n=0}^{N-1} e^{jn\Omega_m} e^{-j\omega_c(\tau_m + \Delta t_m)} \\ &\quad \times \Lambda_m(t - \tau_m - \Delta t_m - nT). \end{aligned} \quad (9)$$

where  $*$  denotes convolution and  $\Lambda_m(\cdot)$  is the auto-correlation of the  $m$ th waveform given by

$$\begin{aligned} \Lambda_m(t) &= \tilde{u}_m(t) * \tilde{u}_m(-t) \\ &= \int_0^{T_p} \tilde{u}_m(t') \tilde{u}_m^*(t' - t) dt'. \end{aligned} \quad (10)$$

This output is sampled with a period that equals to the pulse duration  $T_p$ . Let us assume that  $T$  is an integer multiple of  $T_p$ , i.e.,  $T = \Gamma \times T_p$  where  $\Gamma \in \mathbb{Z}^+$ .  $\Gamma \times N$  samples of this discrete time vector sequence is given by

$$\begin{aligned} \mathbf{z}_m[\gamma] &= \mathbf{z}_m(\gamma T_p), \quad \gamma = 1, \dots, \Gamma \times N, \\ &= \alpha_m s(\Delta t_m) \mathbf{s}_s(\theta) \mathbf{s}_t(\tau_m, \Omega_m)^T \\ &\quad \times \begin{bmatrix} \Lambda_m(\gamma T_p - \tau_m - \Delta t_m) \\ \Lambda_m(\gamma T_p - \tau_m - \Delta t_m - T) \\ \vdots \\ \Lambda_m(\gamma T_p - \tau_m - \Delta t_m - (N-1)T) \end{bmatrix}, \end{aligned} \quad (11)$$

where

$$s(\Delta t_m) \triangleq e^{-j\omega_c \Delta t}, \quad (12)$$

$$\mathbf{s}_t(\tau', \Omega') \triangleq e^{-j\omega_c \tau'} \times \left[ 1, e^{j\Omega'}, \dots, e^{j(N-1)\Omega'} \right]^T. \quad (13)$$

The term  $\mathbf{s}_t$  will be referred to as the temporal steering vector.

Next, this vector sequence is arranged as a cube by folding the two dimensional data array in (11) in lengths of  $\Gamma$  samples. The  $n$ th layer of the resulting cube corresponds to the samples collected between the  $n$ th and the following pulse, i.e.,

$$\mathbf{C}_m[n] \triangleq \left[ \mathbf{z}_m[n\Gamma], \mathbf{z}_m[n\Gamma + 1], \dots, \mathbf{z}_m[(n+1)\Gamma - 1] \right]$$

<sup>1</sup>Perfect orthogonality of waveforms might not be achievable in practice, nevertheless, design of waveforms with a fairly small mutual cross-correlation has been a productive research area which is also discussed, for example, in [19, Chp.2].

This processing chain is illustrated in Fig. 3 together with the cube  $\mathbf{C}_m[n]$  which is also known as the radar data cube [3]. The axes of this cube are array index, slow time and fast time. In the fast time axis, we have  $\Gamma$  samples of the filter output, each of which is associated with a time delay of the reflected signal. These time delays correspond to time of flights which can easily be converted to range values using (4). As a result,  $N$  array measurements from range bin  $r$  is a slice along the slow time axis given by

$$\begin{aligned} \tilde{\mathbf{z}}_m(r) &\triangleq \left[ \mathbf{z}_m[r], \mathbf{z}_m[\Gamma + r], \dots, \mathbf{z}_m[(N-1)\Gamma + r] \right] \\ &= \alpha_m s(\Delta t_m) \mathbf{s}_s(\theta) \mathbf{s}_t(\tau_m, \Omega_m)^T \\ &\quad \times \Lambda_m(rT_p - \tau_m - \Delta t_m). \end{aligned} \quad (14)$$

For convenience regarding the notation in the rest of this article, we stack columns of  $\tilde{\mathbf{z}}_m(r)$  and form a  $LN \times 1$  data vector. Before specifying this vector, let us combine the signal model in a single entity as a function of the reflector kinematic state  $X$  which induces the signals and the range bin  $r$  which is the measurement index:

$$\begin{aligned} \mathbf{s}_m(r, X) &\triangleq s(\Delta t_m) \mathbf{s}_s(\theta(X)) \otimes \mathbf{s}_t(\tau_m(X), \Omega_m(X)) \\ &\quad \times \Lambda_m(rT_p - \tau_m(X) - \Delta t_m) \end{aligned} \quad (15)$$

where  $\otimes$  denotes the Kronecker product operator. Here,  $X = [x, \dot{x}, \ddot{x}, \dot{y}]$  is related to the data vector through the associated time of flight  $\tau_m$  and  $(R, \theta, \Omega_m)$  found by evaluating (3)–(6). The  $r$ th column measurement vector for the hypotheses that a reflector object exist at  $X$  and the null hypothesis are hence given by

$$\mathbf{Z}_m(r) = \begin{cases} \alpha_m \mathbf{s}_m(r, X) + \mathbf{n}_m(r) & , H_1 \text{ holds}, \\ \mathbf{n}_m(r) & , H_0 \text{ holds}, \end{cases} \quad (16)$$

where  $\mathbf{n}_m(r) \sim \mathcal{CN}(\cdot; \mathbf{0}, \Sigma_m)$  models the noise background of the  $m$ th channel and is a complex Gaussian random variable with zero mean and covariance of  $\Sigma_m$ .

Note that, for the (local) mono-static channel  $m = 1$ , and, (16) is found for  $\tau_m = 2R/c$  and the synchronisation term  $\Delta t_m = 0$  in (15). For  $m > 1$ , the measurement vectors are associated with the (remote) bi-static channels, and  $\Delta t_m$  is non-zero and unknown.

## B. Problem definition

We would like to perform a hypothesis test based on the measurement model in (16). These measurements are complex numbers and we are interested in the evaluation of the sufficient statistics for the two hypothesis. Detection/processing using complex measurements are often referred to as coherent detection/processing and conventionally the input is the same resolution bin over multiple pulse returns [3]. Therefore, in order for this operation to maintain coherence, the target position should not be changed.

In order to extend coherent processing to the case of manoeuvring objects and remote transmitters, we introduce the mathematical statement of the problem as evaluation of a likelihood-ratio  $\lambda$  using complex versions of measurements (as

opposed to, for example, using only their moduli) for all  $M$  reflection channels, and, ii) for a time window of  $K$  CPIs given an object trajectory  $\{X_k\}_{k=1}^K$  where  $X_k = [x_k, y_k, \dot{x}_k, \dot{y}_k]^T$  is the object kinematic state at the  $k$ th CPI. This likelihood ratio will then be tested against a threshold in a Neyman-Pearson sense [23, Chp.3]. The detector we consider hence takes the form

$$L(\mathbf{Z}_{1:1:K}, \dots, \mathbf{Z}_{M,1:K} | X_{1:K}, \boldsymbol{\alpha}, \Delta t) \stackrel{H_1}{\gtrless} \stackrel{H_0}{\lessgtr} \mathcal{T} \quad (17)$$

where  $\mathbf{Z}_{m,1:K}$  are the data cubes for channel  $m$  over  $k = 1, \dots, K$ . Here,  $\boldsymbol{\alpha}$  and  $\Delta t$  are reflectivity and synchronisation vectors across the channels, respectively, defined by

$$\begin{aligned} \boldsymbol{\alpha} &\triangleq [\alpha_{1,1}, \dots, \alpha_{1,K}, \dots, \alpha_{M,1}, \dots, \alpha_{M,K}], \\ \Delta t &\triangleq [\Delta t_1, \Delta t_2, \dots, \Delta t_M]. \end{aligned}$$

In order to carry out the test in (17), the trajectory  $X_{1:K}$  needs to be estimated. This is also referred to as tracking and is the subject of Section III along with estimation of the reflection coefficients  $\boldsymbol{\alpha}$ . Algorithmic strategies for estimating the synchronisation term  $\Delta t$  are introduced in Section IV. These results are combined in Section V and threshold selection is detailed in order to evaluate the detection test in (17).

### C. Sufficient statistics for the likelihood ratio

The likelihood ratio on the left hand side of (17) factorises over as the noise samples for different CPIs are also independent. Each time term also factorises over channel likelihood ratios as the related parameters are independent, i.e.,

$$L = \prod_{k=1}^K \prod_{m=1}^M \frac{l(\mathbf{Z}_{m,k} | X_k, \alpha_{m,k}, \Delta t_m, H = H_1)}{l(\mathbf{Z}_{m,k} | X_k, \Delta t_m, H = H_0)}. \quad (18)$$

These measurements also satisfy a locality property in that the number of range bins which are associated with  $X_k$  is limited by the support of  $\Lambda$  in (10) which is of duration  $2T_p$ . Let us define the (range) extend of an object as

$$\mathcal{E}_m(X_k) = \begin{cases} \{r_{m,k}, r_{m,k} + 1\}, & r_{m,k} T_p < \tau_m(X_k) + \Delta t_m \\ \{r_{m,k}\}, & r_{m,k} T_p = \tau_m(X_k) + \Delta t_m \\ \{r_{m,k} - 1, r_{m,k}\}, & r_{m,k} T_p > \tau_m(X_k) + \Delta t_m \end{cases} \quad (19)$$

where

$$r_{m,k} \triangleq \left\lceil \frac{\tau_m(X_k) + \Delta t_m}{T_p} \right\rceil, \quad (20)$$

with  $\lceil \cdot \rceil$  denoting the nearest integer function, and  $\tau_m(X_k) + \Delta t_m$  gives the time of flight in the  $m$ th channel associated with the object state  $X_k$ . This range bin has the highest signal-to-noise ratio (in the  $m$ th channel) given that  $\Lambda$  as a time auto-correlation function typically vanishes towards tails.

As a result, the likelihood ratio in (18) further decomposes into factors over range bins as

$$L = \prod_{k=1}^K \prod_{m=1}^M \prod_{r \in \mathcal{E}_m(X_k)} \frac{l(\mathbf{Z}_{m,k}(r) | X_k, \alpha_{m,k}, \Delta t_m, H = H_1)}{l(\mathbf{Z}_{m,k}(r) | H = H_0)}, \quad (21)$$

The numerator terms in (21) can easily be found using the distribution of the noise in the signal model in (16) as

$$\begin{aligned} l(\mathbf{Z}_{m,k}(r) | X_k, \alpha_{m,k}, \Delta t_m, H = H_1) \\ = \mathcal{CN}(\mathbf{Z}_{m,k}(r); \alpha_{m,k} \mathbf{s}_m(r, X_k), \Sigma_m). \end{aligned} \quad (22)$$

The denominator in (21) regarding the noise only hypothesis is nothing but the noise density evaluated at  $\mathbf{Z}_{m,k}(r)$ . Therefore, the instantaneous likelihood ratio in (21) after substituting from (22) and the noise distribution is found as

$$\begin{aligned} l(\mathbf{Z}_{m,k}(r) | X_k, \alpha_{m,k}, \Delta t_m) \\ \triangleq \frac{\mathcal{CN}(\mathbf{Z}_{m,k}(r); \alpha_{m,k} \mathbf{s}_m(r, X_k), \Sigma_m)}{\mathcal{CN}(\mathbf{Z}_{m,k}(r_{m,k}); \mathbf{0}, \Sigma_m)} \\ = \exp \left\{ 2 \operatorname{Re} \{ \alpha_{m,k}^* \mathbf{s}_m(r, X_k)^H \Sigma_m^{-1} \mathbf{Z}_{m,k}(r) \} \right\} \\ \times \exp \left\{ - |\alpha_{m,k}|^2 \mathbf{s}_m(r, X_k)^H \Sigma_m^{-1} \mathbf{s}_m(r, X_k) \right\}, \end{aligned} \quad (23)$$

where  $(\cdot)^H$  is the Hermitian of its argument,  $\operatorname{Re}\{\cdot\}$  takes the real part of its complex argument,  $(\cdot)^*$  denotes conjugate and  $|\cdot|$  denotes modulus of a complex variable, respectively.

The likelihood ratio evaluation given in (23) is advantageous in that only a linear operation needs to be performed on the measurements which is in the form of a whitening transform with the inverse noise covariance followed by an inner product with the signal model. Because the signal model involves the spatial steering vector in (7), this inner product effectively performs beamforming on the measurements filtering out contributions of other objects at the same range. Note that a second filtering is with respect to the Doppler as the temporal steering vector (13) is also in the signal model.

## III. SIMULTANEOUS TRACKING AND REFLECTION COEFFICIENT ESTIMATION

In this section, we consider estimation of the object trajectory  $X_{1:K}$  using coherent pulse returns during a CPI. Object trajectories are modelled as random vector sequences generated by a Markov state space model [24], i.e.,

$$X_{1:K} \sim p(X_1) \prod_{k=2}^K p(X_k | X_{k-1}), \quad (24)$$

where the Markov transition density is selected as

$$\begin{aligned} p(X_k | X_{k-1}) &= \mathcal{N}(X_k; F X_{k-1}, Q) \\ F &= \begin{bmatrix} 1 & 0 & \Delta & 0 \\ 0 & 1 & 0 & \Delta \\ 0 & 0 & 1 & 0 \\ 0 & 0 & 0 & 1 \end{bmatrix}, \end{aligned} \quad (25)$$

where  $\Delta$  is the time interval between two consecutive CPIs,  $F$  models constant velocity motion, and  $Q$  is the covariance matrix specifying the level of the process noise modelling unknown manoeuvres.

The initial distribution  $p(X_1)$  is selected as a uniform distribution over the range-bearing interval for the detection test. These intervals often correspond to radar specific resolution

bins. Let us denote the corresponding bounded set in the state space by  $\mathcal{B}$ , and a uniform distribution on  $\mathcal{B}$  by  $U_{\mathcal{B}}$ . Therefore,

$$p(X_1) = U_{\mathcal{B}}(X_1). \quad (26)$$

Sequential estimation of  $X_{1:K}$  as data cubes arrive is performed using Bayesian recursive filtering [24]. Suppose we have the given distribution of the state variable at step  $k-1$  based on all the measurements collected up to and including CPI  $k-1$ , i.e.,  $p(X_{k-1}|\mathbf{Z}_{1:k-1})$ . In order to update this prior information with the measurement at the  $k$ th CPI, first, the Chapman-Kolmogorov equation is realised and a prediction density is found as

$$p(X_k|\mathbf{Z}_{1:k-1}) = \int p(X_k|X_{k-1})p(X_{k-1}|\mathbf{Z}_{1:k-1})dX_{k-1}, \quad (27)$$

where the first term inside the integral is the Markov transition given by (25).

The update stage of filtering is given by the multiplication of this prediction with the measurement likelihood and marginalising out all other variables, i.e.,

$$p(X_k|\mathbf{Z}_{1:k}) \propto \int_{\alpha_k} \int_{\Delta t} l(\mathbf{Z}_k|X_k, \alpha_k, \Delta t) \times p(\alpha_k)p(\Delta t)p(X_k|\mathbf{Z}_{1:k-1})d\alpha_k d\Delta t, \quad (28)$$

where  $p(\alpha_k)$  and  $p(\Delta t)$  are prior densities for the reflection coefficient and the synchronisation term, respectively.

The measurement likelihood in (28) is nothing but the product of the numerator terms in the likelihood ratio in (21) over the object's range extend and channels for time step  $k$ , i.e.,

$$l(\mathbf{Z}_k|X_k, \alpha_k, \Delta t) \propto \prod_{m=1}^M \prod_{r \in \mathcal{E}_m(X_k)} l(\mathbf{Z}_{m,k}(r)|X_k, \alpha_{m,k}, \Delta t_m, H = H_1) \quad (29)$$

and is easily computed by evaluating complex Gaussian densities as discussed in Section II-C.

The marginalisation of the reflection coefficients and synchronisation terms, however, is not straightforward: First, one needs to select prior densities for these terms. One reasonable approach is to use a non-informative prior such as Jeffrey's prior [25, Chp.5]. These priors are useful when they lead to tractable computations in (28) (see, e.g., [26]). In our problem setting, however, Jeffrey's priors for the reflection coefficients and the synchronisation terms are constant, and, do not help in finding a tractable form for the full Bayesian update in (28).

In order to tackle this challenge, we use an empirical Bayes approach [17]. These methods approximate the integration in (28) by solving an optimisation problem for finding the likely values of the unknowns and evaluating the integrand at those values. In other words, (28) is rewritten as

$$p(X_k|\mathbf{Z}_{1:k}) = \int_{\alpha_k} \int_{\Delta t} p(X_k|\mathbf{Z}_{1:k}, \alpha_k, \Delta t)p(\alpha_k, \Delta t|\mathbf{Z}_{1:k})d\alpha_k d\Delta t. \quad (30)$$

Here, the reflection coefficients and the synchronisation terms act as model parameters to be selected and the second

term inside the integration is similar to a prior for them. Because this prior is conditioned on the measurements, more probability mass should be concentrating around the maximum likelihood (ML) estimates of these values. Let us select this density as

$$\begin{aligned} p(\alpha_k, \Delta t|\mathbf{Z}_{1:k}) &= p(\alpha_k|\mathbf{Z}_{1:k})p(\Delta t|\mathbf{Z}_{1:k}) \\ p(\alpha_k|\mathbf{Z}_{1:k}) &\leftarrow \delta_{\hat{\alpha}_k}(\alpha_k) \\ p(\Delta t|\mathbf{Z}_{1:k}) &\leftarrow \delta_{\hat{\Delta t}}(\Delta t), \end{aligned} \quad (31)$$

where  $\leftarrow$  denotes assignment and  $\delta$  is Dirac's delta distribution. In other words, we select the model densities given the measurements as a Dirac's delta distribution concentrated around their ML estimates  $\hat{\alpha}_k$  and  $\hat{\Delta t}$ , respectively.

After substituting from the empirical priors in (31) into (30), one obtains the empirical Bayes update as

$$p(X_k|\mathbf{Z}_{1:k}) \propto l(\mathbf{Z}_k|X_k, \hat{\alpha}_k, \hat{\Delta t})p(X_k|\mathbf{Z}_{1:k-1}) \quad (32)$$

where  $\propto$  denotes approximate proportionality. The approximation accuracy is better when these ML estimates are obtained using informative likelihoods (as quantified by their Fisher information) and equivalently have small CRLBs.

We detail ML estimation of the reflection coefficients  $\alpha$  and the synchronisation term in Section IV. For the remaining part of this section, let us assume that these estimates are given.

For realising the recursive filtering, a sequential Monte Carlo (SMC) approach known as the particle filter is used [27]. In particular, we use a bootstrap filtering approach for estimating the object trajectory.

The prediction stage at time step  $k=1$  is realised by forming a regular grid of  $P$  points over  $\mathcal{B}$  representing samples generated from the initial state distribution in (26). These points constitute an equally weighted set of particles. For  $k > 1$  we will have found weighted samples, or, particles, representing the state posterior in the previous step. Let us denote this set by

$$\left\{ X_{k|k-1}^{(p)}, \zeta_{k|k-1}^{(p)} \right\}_{p=1}^P,$$

where  $\zeta_{k|k-1}^{(p)}$  is the weight of the  $p$ th sample. The prediction stage is then realised by sampling from the Markov transition as

$$X_{k|k-1}^{(p)} \sim p(\cdot|X_{k-1}^{(p)}), \quad p = 1, \dots, P. \quad (33)$$

The weights of these samples in the particle set  $\{X_{k|k-1}^{(p)}, \zeta_{k|k-1}^{(p)}\}$  is given by

$$\zeta_{k|k-1}^{(p)} = \zeta_{k-1}^{(p)},$$

in order for this set to represent the prediction density in (27).

In the update stage, the same sample set is used to represent the state posterior in (32). The weights of the samples need to be adjusted using the measurement likelihood, i.e.,

$$\zeta_k^{(p)} = \frac{\tilde{\zeta}_k^{(p)}}{\sum_{p'=1}^P \tilde{\zeta}_k^{(p')}}, \quad (34)$$

$$\tilde{\zeta}_k^{(p)} = \zeta_{k|k-1}^{(p)} l(\mathbf{Z}_k|X_k = X_{k|k-1}^{(p)}, \hat{\alpha}_k, \hat{\Delta t}), \quad (35)$$

After finding the normalised weights in (34), we test degeneracy of the weighted particles. The degeneracy test is performed by finding the number of effective particles using

$$N_{eff} = \frac{1}{\sum_{p=1}^P \left( \zeta_k^{(p)} \right)^2}, \quad (36)$$

and, comparing it with a threshold  $\mathcal{T}_{eff}$ . When  $N_{eff} < \mathcal{T}_{eff}$ , we perform re-sampling (see, e.g., [27]) and continue filtering with a new equally weighted sample set.

Using the above particle filter, the object state  $X_k$  at the  $k$ th CPI is estimated by using the empirical weighted average

$$\hat{X}_k = \sum_{p=1}^P \zeta_k^{(p)} X_{k|k-1}^{(p)}, \quad (37)$$

where  $\hat{X}_k$  denotes the estimated object state  $X_k$ .

#### IV. ML ESTIMATION OF THE MODEL PARAMETERS

In this section, we first introduce the ML estimator for the reflection coefficients. This estimator is an iterative algorithm realising Expectation Maximisation used in Section III– in particular when evaluating the tracking update in (35)–and, is also central to long time integration detailed later in Section V. Then, we derive the ML synchronisation term estimator used together with the reflectivity estimator in Section III.

##### A. ML estimation of the reflection coefficients

The reflection coefficients associated with an object at state  $X_k$  are constant for the duration of a CPI and vary across consecutive CPIs due to the change of the object position, orientation etc. Let us consider a likelihood of the reflection coefficients with taking into account the measurement likelihood at the  $k$ th CPI in (29). This likelihood can be found by marginalising out all other variables together with the measurement likelihood. However, we do not have the complete information on these variables to find the reflection coefficients. Thus, we propose an approach which computes the expectation of the log-measurement likelihood with respect to the unknown variables given the measurements and finds the reflection coefficients which maximise the expected log-likelihood. This approach is referred to as an expectation–maximisation (EM) algorithm [16]. This is an iterative algorithm comprised of an expectation stage and a maximisation stage at each iteration.

Let us define  $\boldsymbol{\alpha}^{(i)} = \{\alpha_m^{(i)}\}_{m=1}^M$  which is the set of the reflection coefficients in  $M$  reflection channels at the  $i$ th iteration for  $i = 1, 2, \dots$ . In the expectation stage, we define a  $Q$  function with taking into account the natural logarithm of the measurement likelihood in (29) in order to realise the expectation of the log-likelihood. Here, we assume that all unknown variables in the measurement likelihood are independent, and, the ML estimate of the synchronisation term and  $\boldsymbol{\alpha}^{(i-1)}$  at the  $i-1$ th iteration are given. When  $i = 1$ , we set

the initial values for  $\boldsymbol{\alpha}^{(0)}$ . The  $Q$  function<sup>2</sup> at the  $i$ th iteration is hence found as

$$\begin{aligned} Q(\boldsymbol{\alpha}_k | \boldsymbol{\alpha}^{(i-1)}) &= \int_{X_k} \log(l(\mathbf{Z}_k | X_k, \boldsymbol{\alpha}_k, \Delta\hat{\mathbf{t}}) p(X_k | \mathbf{Z}_{1:k-1})) \\ &\quad \times p(X_k | \mathbf{Z}_{1:k}, \boldsymbol{\alpha}^{(i-1)}, \Delta\hat{\mathbf{t}}) dX_k \\ &\propto \int_{X_k} \log l(\mathbf{Z}_k | X_k, \boldsymbol{\alpha}_k, \Delta\hat{\mathbf{t}}) p(X_k | \mathbf{Z}_{1:k}, \boldsymbol{\alpha}^{(i-1)}, \Delta\hat{\mathbf{t}}) dX_k \\ &\propto \mathbb{E}\{\log l(\mathbf{Z}_k | X_k, \boldsymbol{\alpha}_k, \Delta\hat{\mathbf{t}}) | \mathbf{Z}_{1:k}, \boldsymbol{\alpha}^{(i-1)}\}, \end{aligned} \quad (38)$$

where  $\mathbb{E}$  denotes the expectation of  $\log l(\cdot)$  with respect to  $p(X_k | \mathbf{Z}_{1:k}, \boldsymbol{\alpha}^{(i-1)}, \Delta\hat{\mathbf{t}})$ . Here,  $\Delta\hat{\mathbf{t}}$  is the ML estimate of the synchronisation term. The details of this ML estimation will be introduced in Section IV-B.

The prior  $p(X_k | \mathbf{Z}_{1:k}, \boldsymbol{\alpha}^{(i-1)}, \Delta\hat{\mathbf{t}})$  in (38) is found as

$$\begin{aligned} p(X_k | \mathbf{Z}_{1:k}, \boldsymbol{\alpha}^{(i-1)}, \Delta\hat{\mathbf{t}}) &= \frac{l(\mathbf{Z}_k | X_k, \boldsymbol{\alpha}^{(i-1)}, \Delta\hat{\mathbf{t}}) p(X_k | \mathbf{Z}_{1:k-1})}{\int_{X_k} p(\mathbf{Z}_k | X_k, \boldsymbol{\alpha}^{(i-1)}, \Delta\hat{\mathbf{t}}) p(X_k | \mathbf{Z}_{1:k-1}) dX_k} \end{aligned} \quad (39)$$

where  $l(\cdot)$  is the measurement likelihood in (29) given  $\boldsymbol{\alpha}^{(i-1)}$ ,  $p(X_k | \mathbf{Z}_{1:k-1})$  is the prediction density in (27), and the denominator is the normalised term.

In our problem setting, we have the set of the state particles  $\{X_{k|k-1}^{(p)}, \zeta_{k|k-1}^{(p)}\}_{p=1}^P$  from the prediction stage at the time step  $k$ . The prior in (39) with taking into account these particles is rewritten as

$$\begin{aligned} p(X_k = X_{k|k-1}^{(p)} | \mathbf{Z}_{1:k}, \boldsymbol{\alpha}^{(i-1)}, \Delta\hat{\mathbf{t}}) &= \frac{l(\mathbf{Z}_k | X_k = X_{k|k-1}^{(p)}, \boldsymbol{\alpha}^{(i-1)}, \Delta\hat{\mathbf{t}}) \zeta_{k|k-1}^{(p)}}{\sum_{p=1}^P l(\mathbf{Z}_k | X_k = X_{k|k-1}^{(p)}, \boldsymbol{\alpha}^{(i-1)}, \Delta\hat{\mathbf{t}}) \zeta_{k|k-1}^{(p)}}, \end{aligned} \quad (40)$$

and we define  $\Gamma_p^{(i-1)} \triangleq p(X_k = X_{k|k-1}^{(p)} | \mathbf{Z}_{1:k}, \boldsymbol{\alpha}^{(i-1)}, \Delta\hat{\mathbf{t}})$  for  $p = 1, \dots, P$ .

The  $Q$  function in (38) with taking into account (40) hence approximates to

$$Q(\boldsymbol{\alpha}_k | \boldsymbol{\alpha}^{(i-1)}) \approx \sum_{p=1}^P \Gamma_p^{(i-1)} \log l(\mathbf{Z}_k | X_k = X_{k|k-1}^{(p)}, \boldsymbol{\alpha}_k, \Delta\hat{\mathbf{t}}). \quad (41)$$

Next, we find  $\boldsymbol{\alpha}_k$ , which maximises the  $Q$  function in (41) by solving

$$\hat{\boldsymbol{\alpha}}_k = \arg \max_{\boldsymbol{\alpha}_k} \sum_{p=1}^P \Gamma_p^{(i-1)} \log l(\mathbf{Z}_k | X_k = X_{k|k-1}^{(p)}, \boldsymbol{\alpha}_k, \Delta\hat{\mathbf{t}}), \quad (42)$$

where  $\hat{\boldsymbol{\alpha}}_k$  is the ML estimate of  $\boldsymbol{\alpha}_k$ .

For solving (42), we first take the natural logarithm of the likelihood in (29) with taking into account the instantaneous likelihood in (22) and obtain (43) (see the top of the next page).

Afterwards, we take the first order partial derivative of (43) with respect to  $\alpha_{m,k}$  in order to find the reflection coefficient in the  $m$ th reflection channel and set this result equal to zero.

<sup>2</sup>The details of a  $Q$  function in state space are explained in [16]

$$Q(\boldsymbol{\alpha}_k | \boldsymbol{\alpha}^{(i-1)}) = \sum_{p=1}^P \Gamma_p^{(i-1)} \left[ \sum_{m=1}^M \sum_{r \in \mathcal{E}_m(X_{k|k-1}^{(p)})} \left( -\log(\pi^{LN} \det(\Sigma_m)) - \mathbf{Z}_{m,k}(r)^H \Sigma_m^{-1} \mathbf{Z}_{m,k}(r) \right. \right. \\ \left. \left. + 2 \operatorname{Re}\{\alpha_{m,k}^* \mathbf{s}_m(r, X_{k|k-1}^{(p)})^H \Sigma_m^{-1} \mathbf{Z}_{m,k}(r)\} - |\alpha_{m,k}|^2 \mathbf{s}_m(r, X_{k|k-1}^{(p)})^H \Sigma_m^{-1} \mathbf{s}_m(r, X_{k|k-1}^{(p)}) \right) \right] \quad (43)$$

$$\frac{\partial Q(\boldsymbol{\alpha}_k | \boldsymbol{\alpha}^{(i-1)})}{\partial \alpha_{m,k}} = 0 \\ \hat{\alpha}_{m,k} = \frac{\sum_{p=1}^P \sum_{r \in \mathcal{E}_m(X_{k|k-1}^{(p)})} \Gamma_p^{(i-1)} \mathbf{s}_m(r, X_{k|k-1}^{(p)})^H \Sigma_m^{-1} \mathbf{Z}_{m,k}(r)}{\sum_{p=1}^P \sum_{r \in \mathcal{E}_m(X_{k|k-1}^{(p)})} \Gamma_p^{(i-1)} \mathbf{s}_m(r, X_{k|k-1}^{(p)})^H \Sigma_m^{-1} \mathbf{s}_m(r, X_{k|k-1}^{(p)})} \quad (44)$$

**Algorithm 1** Expectation-maximisation algorithm for estimating the reflection coefficients

- 1: Initialisation: Chooses initial values of  $\boldsymbol{\alpha}^{(0)}$
- $\boldsymbol{\alpha}^{(0)} = \{\alpha_m^{(0)}\}_{m=1}^M$  and  $i = 0$
- 2: **while**  $\|\hat{\boldsymbol{\alpha}}^i - \boldsymbol{\alpha}^{(i-1)}\| > \epsilon$  (i.e., convergence test) **do**
- 3:    $i \leftarrow i + 1$
- 4:   Expectation stage:
- 5:   Compute  $\Gamma_p^{(i-1)}$  in (40) given  $\boldsymbol{\alpha}^{(i-1)}$
- 6:   Maximisation stage:
- 7:   Find  $\hat{\boldsymbol{\alpha}}_k$  using (44)
- 8:    $\boldsymbol{\alpha}^i \leftarrow \hat{\boldsymbol{\alpha}}_k$
- 9: **end while**
- 10: Find  $\hat{\boldsymbol{\alpha}}_k = \boldsymbol{\alpha}^i$

As a result, the ML estimate of  $\alpha_{m,k}$  in the  $m$ th reflection channel is found as (44) (see the top of the next page). Here, this proposed estimator simultaneously performs the digital beam-forming and estimation of the Doppler frequency by using  $\mathbf{s}_m(r, X_{k|k-1}^{(p)})$ , which is the noise free signal modelled in (15) associated with  $X_{k|k-1}^{(p)}$ . Therefore, this approach has a capability that separately estimates the reflection coefficient from each object, when there are multiple objects located in the same range bin with different angles of arrival.

After finding  $\hat{\boldsymbol{\alpha}}_k = \{\hat{\alpha}_{m,k}\}_{m=1}^M$  based on (44) for  $M$  reflection channels, we test convergence by computing  $\|\hat{\boldsymbol{\alpha}}_k - \boldsymbol{\alpha}^{(i-1)}\|$  with  $\|\cdot\|$  denoting Euclidean norm, and, comparing its result with a threshold  $\epsilon$ . When  $\|\hat{\boldsymbol{\alpha}}_k - \boldsymbol{\alpha}^{(i-1)}\| > \epsilon$ , we assign  $\boldsymbol{\alpha}^{(i-1)} \leftarrow \hat{\boldsymbol{\alpha}}_k$  and repeat the expectation stage in (41) and the maximisation stage in (42). In the other case, we have the reflection coefficients as  $\hat{\boldsymbol{\alpha}}_k$ . The overall process of the proposed EM algorithm is expressed in Algorithm 1.

Next, we consider Cramér-Rao low bound (CRLB) which provides the theoretical minimum variance for an unbiased estimator. In our problem setting, we find CRLB with respect to the  $m$ th complex reflection coefficient by using inverse Fisher information. The Fisher information is found by taking the second order partial derivative of a likelihood for the reflection coefficients with respect to the reflection coefficient

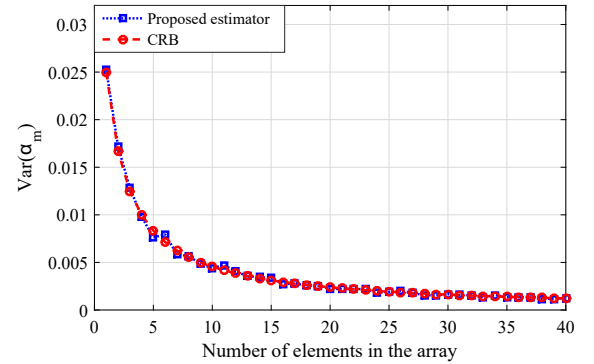


Fig. 4. Cramér-Rao bound compared to the variance obtained by using the proposed estimator for the complex reflection coefficient: CRLB (red line) and the variance using the proposed estimator (blue line) with an  $-6\text{dB}$  SNR object versus the number of elements in array.

<sup>3</sup>. This likelihood is found as

$$l(\mathbf{Z} | \boldsymbol{\alpha}) = \int_X \int_{\Delta t} l(\mathbf{Z} | X, \boldsymbol{\alpha}, \Delta t) p(X) p(\Delta t) dX d\Delta t, \quad (45)$$

where  $l(\cdot)$  is the measurement likelihood in (29), and,  $p(X)$  and  $p(\Delta t)$  are the priors of  $X$  and  $\Delta t$ , respectively. We assume that we have the full knowledge of  $X$  and  $\Delta t$  in order to find the Fisher information. The Fisher information after substituting  $X^T$  and  $\Delta t^T$  as the true values of  $X$  and  $\Delta t$  in the natural logarithm of the likelihood given in (45) is hence found as

$$\mathbf{I}(\alpha_m) = -\mathbb{E} \left\{ \frac{\partial^2 \log l(\mathbf{Z} | \boldsymbol{\alpha})}{\partial \alpha_m^2} \right\} \\ = -\mathbb{E} \left\{ \frac{\partial^2 \log l(\mathbf{Z} | X = X^T, \boldsymbol{\alpha}, \Delta t = \Delta t^T)}{\partial \alpha_m^2} \right\} \quad (46) \\ = 2 \sum_{r \in \mathcal{E}_m(X^T)} \mathbf{s}_m(r, X^T)^H \Sigma_m^{-1} \mathbf{s}_m(r, X^T), \quad (47)$$

where  $\mathbf{I}(\alpha_m)$  is the Fisher information of the  $m$ th reflection coefficient, and  $\mathbb{E}\{\cdot\}$  denotes the expectation of its input argument. As a result, CRLB using  $\mathbf{I}(\alpha_m)$  in (47) is found as

$$\operatorname{Var}(\hat{\alpha}_m) \geq \mathbf{I}(\alpha_m)^{-1} \\ = \frac{1}{2 \sum_{r \in \mathcal{E}_m(X^T)} \mathbf{s}_m(r, X^T)^H \Sigma_m^{-1} \mathbf{s}_m(r, X^T)} \quad (48)$$

where  $\operatorname{Var}(\hat{\alpha}_m) = \mathbb{E}\{|\alpha_m - \hat{\alpha}_m|^2\}$  is the variances of the complex reflection coefficient.

<sup>3</sup>The derivation of the Fisher information for the reflection coefficient is given in Appendix B

For evaluating our proposed estimator, we set  $N = 10$  transmitted pulses in a CPI and generate 500 measurements using (16) with an  $-6\text{dB}$  SNR object. We then estimate the complex reflection coefficient using in Algorithm 1 with the true synchronisation term and  $P$  samples generated by using uniform distribution on a small boundary of the true value  $X$  in (26).

Fig. 4 illustrates the CRLB of the  $m$ th complex reflection coefficient (red line) determined by using (48), and, the variance obtained by using our proposed EM estimator (blue line) in Algorithm 1 in accordance with increasing elements in the array. For the accuracy of estimating the reflection coefficient using the ULA structure, it is shown that the variance of the estimated reflection coefficient becomes lower when increasing the elements in the array. It is also clearly observed that the variance using our proposed estimator is matched with the CRLB. We will demonstrate the efficacy of our proposed estimator based on estimating the object trajectory  $X_{1:K}$  and the synchronisation terms  $\Delta t$  in comparison with results when having full knowledge of the object trajectory and the synchronisation term in Section (VI).

### B. Synchronisation of the detector with the remote transmitters

Let us consider estimation of unknown time shifts as the synchronisation terms in the reflection channels. The proposed approach is to use the bi-static configuration in which the ULA receiver utilises a digital beam-forming to simultaneously divert beams to collect both the reflected and the direct signals when the omni-directional transmitter is used. Therefore, the received signal in the  $m$ th direct channel contains an unknown time shift  $\Delta t_m$ , which is equivalent to  $\Delta t_m$  received in the  $m$ th reflection channel. We would like to estimate the unknown time shifts by maximising a likelihood of the direct channels.

For this purpose, we consider the signal received through direct channels. When the receiver collects the direct signal emitted by the  $m$ th transmitter located at  $X_m = [x_m, y_m, 0, 0]^T$ , the measurement in the  $m$ th direct channel is obtained by using (8)–(15). The measurement vector at the  $r$ th range bin in a CPI after sampling the  $m$ th matched filter output (which corresponds to the  $m$ th direct channel) is hence found as

$$\mathbf{Z}_m(r) = \sqrt{E_m} \tilde{\mathbf{s}}_m(r, X_m) + \mathbf{n}_m(r). \quad (49)$$

Here,  $E_m$  is the known received energy in the  $m$ th direct channel at the receiver front-end, and  $\tilde{\mathbf{s}}_m(\cdot)$  is the noise free signal model associated with the location  $X_m$  of the  $m$ th transmitter with the zero angular Doppler frequency, i.e.,

$$\begin{aligned} \tilde{\mathbf{s}}_m(r, X_m) &\triangleq s(\Delta t_m) \mathbf{s}_s(\theta_m(X_m)) \otimes \mathbf{s}_t(\tau(X_m), \Omega = 0) \\ &\quad \times \Lambda_m(rT_p - \tau(X_m) - \Delta t_m), \end{aligned} \quad (50)$$

where  $\mathbf{s}_s$  and  $\mathbf{s}_t$  are the spatial steering vector in (7) and the temporal steering vector in (13), respectively,  $\tau(X_m)$  is the time of flight given by using (4), and  $\theta_m(X_m)$  is the angle of arrival from the receiver to the  $m$ th transmitter defined in (6).

Next, we evaluate the sufficient statistics of the measurement in (49) by using the known location  $X_m$ , i.e.,

$$D_m(r) = \mathbf{h}(X_m)^H \mathbf{Z}_m(r)$$

$$\begin{aligned} &= LN\sqrt{E_m} s(\Delta t_m) \Lambda_m(rT_p - \tau(X_m) - \Delta t_m) \\ &\quad + n_m(r), \end{aligned} \quad (51)$$

where  $n_m(r) = \mathbf{h}(X_m)^H \mathbf{n}_m(r)$  is the noise background of the  $m$ th direct channel and is assumed to be complex Gaussian random variable with zero mean and variance  $\sigma_m^2$ , and  $\mathbf{h}(X_m)$  is the beam-forming factor, i.e.,

$$\mathbf{h}(X_m) \triangleq \mathbf{s}_s(\theta_m(X_m)) \otimes \mathbf{s}_t(\tau_m(X_m), \Omega = 0)$$

which matches the angle of arrival and the time of flight in the  $m$ th direct channel.

In order to find  $\Delta t_m$  in (51), we consider the ML estimation approach with taking into account the measurements from 1 to  $k$ . In our problem setting, the received signal in the  $m$ th direct channel which contains  $\Delta t_m$  after the beam-forming in (51) has  $2T_p$  duration. The corresponding range bins are given by

$$\tilde{\mathcal{E}}_m(X_m) = \begin{cases} \{r_m, r_m + 1\} & r_m T_p < \tau(X_m) + \Delta t_m \\ \{r_m\} & r_m T_p = \tau(X_m) + \Delta t_m \\ \{r_m, r_m - 1\} & r_m T_p > \tau(X_m) + \Delta t_m \end{cases}, \quad (52)$$

where

$$r_m = \left[ \frac{\tau(X_m) + \Delta t_m}{T_p} \right]$$

is the  $r$ th range bin associated with  $\Delta t_m$  with  $[\cdot]$  denoting the nearest integer function. As a result,  $\Delta t_m$  is estimated by solving

$$\begin{aligned} \hat{\Delta t}_m &= \\ \arg \max_{\Delta t_m} \log \prod_{r \in \tilde{\mathcal{E}}_m(X_m)} l(D_{m,1}(r), \dots, D_{m,k}(r) | \Delta t_m), \end{aligned} \quad (53)$$

where  $\tilde{\mathcal{E}}_m(X_m)$  is the set of the range bins defined in (52), and  $l(D_{m,1:k}(r) | \Delta t_m)$  is the measurement likelihood at the  $r$ th range bin in the  $m$ th direct channel given by

$$\begin{aligned} l(D_{m,1:k}(r) | \Delta t_m) &= \left( \frac{1}{\pi \sigma_m^2} \right)^k \\ &\quad \times \exp \left\{ \sum_{\tilde{k}=1}^k -\frac{\tilde{D}_{m,\tilde{k}}(r)^* \tilde{D}_{m,\tilde{k}}(r)}{\sigma_m^2} \right\}, \end{aligned} \quad (54)$$

where

$$\begin{aligned} \tilde{D}_{m,\tilde{k}}(r) &\triangleq \\ D_{m,\tilde{k}}(r) - LN\sqrt{E_m} s(\Delta t_m) \Lambda_m(rT_p - \tau(X_m) - \Delta t_m). \end{aligned}$$

For solving (53), we require to take a first order derivative of the log-likelihood function in (53) with respect to  $\Delta t_m$  and set its result to a zero. This leads to finding  $\Delta t_m$  iteratively because  $\Delta t_m$  involves a phase term and a shift term of the transmitted waveform in the likelihood defined in (54). Instead of taking the derivative of the log-likelihood in (53), we

**Algorithm 2** Maximum likelihood estimation of  $\Delta t_m$  via golden section search

1: Initialisation: Set

$$a = \Delta t_{min}, \quad b = \Delta t_{max}, \quad g = \frac{\sqrt{5} - 1}{2}, \quad \text{and}$$

$$f(\Delta t_m) \triangleq \log \prod_{r \in \mathcal{E}_m(\Delta t_m)} l(D_{m,1:k}(r) | \Delta t_m) \text{ in (53)}$$

```

2: Find  $x_1 = a + (b - a) \times (1 - g)$  and  $x_2 = a + (b - a) \times g$ 
3: Compute  $f(\Delta t_m = x_1)$  and  $f(\Delta t_m = x_2)$ 
4: while  $|x_1 - x_2| > A_c$  (i.e., accuracy of estimation) do
5:   if  $f(x_1) > f(x_2)$  then
6:     Set a new interval  $[a, b = x_2]$ 
7:     Find  $x_1 = a + (b - a) \times (1 - g)$  and  $x_2 = x_1$ 
8:   else
9:     Set a new interval  $[a = x_1, b]$ 
10:    Find  $x_1 = x_2$  and  $x_2 = a + (b - a) \times (g)$ 
11:   end if
12:   Compute  $f(x_1)$  and  $f(x_2)$ 
13: end while
14: if  $f(x_1) > f(x_2)$  then
15:   Select  $\hat{\Delta t}_m = x_1$ 
16: else
17:   Select  $\hat{\Delta t}_m = x_2$ 
18: end if

```

use a golden section search algorithm<sup>4</sup>. This algorithm is a technique to find the maximum value of an objective function by successively narrowing an interval in which the maximum value of the objective function occurs.

For this purpose, we use the log-likelihood in (53) as the objective function  $f(\Delta t_m)$  which is a function of a given  $\Delta t_m$  together with setting the initial interval  $[\Delta t_{min}, \Delta t_{max}]$ . We then choose two points in the interval, which are found by using the golden ratio  $g = \frac{\sqrt{5}-1}{2}$ .

Let us define these two points as  $\{x_1, x_2\}$ , and, find

$$x_1 = \Delta t_{min} + (\Delta t_{max} - \Delta t_{min}) \times (1 - g)$$

and

$$x_2 = \Delta t_{min} + (\Delta t_{max} - \Delta t_{min}) \times g$$

, respectively. We then compute both  $f(\Delta t_m = x_1)$  and  $f(\Delta t_m = x_2)$ . If  $f(\Delta t_m = x_1) > f(\Delta t_m = x_2)$ , the maximum value of the objective function will occur in the interval  $[\Delta t_{min}, \Delta t_{max} = x_2]$ . Otherwise, the maximum value will occur in  $[\Delta t_{min} = x_1, \Delta t_{max}]$ . We iteratively do the above steps until the distance between these points small and select one of these two points which makes the objective function value larger as  $\hat{\Delta t}_m$ . The overall process of the golden section algorithm for finding  $\Delta t_m$  is described in Algorithm 2.

<sup>4</sup>The general properties of the golden section search algorithm are explained in [28, Chp.10]

## V. LONG TIME INTEGRATION FOR DETECTION

### A. Long time integration

In this section, we detail the proposed detection scheme based on the long time integration. This integration enables us to add the complex reflection coefficients in both the mono-static and the bi-static channels for an arbitrary long time with taking into account the object trajectory.

In order to perform the proposed integration, we first estimate  $\Delta t$  using Algorithm 2. Then, we find  $\hat{\alpha}_k$  based on Algorithm 1 after substituting  $\hat{\Delta t}$ . Afterwards, we perform the update stage of SMC recursion after substituting  $\hat{\alpha}_k$  and  $\hat{\Delta t}$  in (35). The object state  $X_k$  is estimated by using (37). As a result, the long time integration after substituting  $\hat{X}_k$ ,  $\hat{\alpha}_k$  and  $\hat{\Delta t}$  in the natural logarithm of the likelihood ratio in (21) for  $k = 1, \dots, K$  CPIs is performed by

$$\begin{aligned} \log L(\mathbf{Z}_{1:K}(\mathcal{E}_m(\hat{X}_{1:K})) | \hat{X}_{1:K}, \hat{\alpha}_{1:K}, \hat{\Delta t}) = \\ \sum_{k=1}^K \sum_{m=1}^M \sum_{r \in \mathcal{E}_m(\hat{X}_k)} \left( 2\text{Re}\{\hat{\alpha}_{m,k}^* \mathbf{s}_m(r, \hat{X}_k)^H \Sigma_m^{-1} \mathbf{Z}_{m,k}(r)\} \right. \\ \left. - |\hat{\alpha}_{m,k}|^2 \mathbf{s}_m(r, \hat{X}_k)^H \Sigma_m^{-1} \mathbf{s}_m(r, \hat{X}_k) \right) \end{aligned} \quad (55)$$

where  $\mathcal{E}_m(\hat{X}_k)$  is the set of range bins in the  $m$ th channel in (19). We find that this proposed integration performs coherent integration of  $\mathcal{E}_m(\hat{X}_k) \times L \times N$  samples in a CPI for each channel together with continuing non-coherent integration across the channels as well as consecutive CPIs, while taking into account the estimated object trajectory  $\hat{X}_{1:K}$ .

The object detection is performed by comparing the aforementioned log-likelihood ratio to a detection threshold, i.e.,

$$\log L(\mathbf{Z}_{1:K}(\mathcal{E}_m(\hat{X}_{1:K})) | \hat{X}_{1:K}, \hat{\alpha}_{1:K}, \hat{\Delta t}) \stackrel{H_1}{\geq} \log \mathcal{T}_K, \quad (56)$$

where  $\log \mathcal{T}_K$  is the detection threshold for a given constant false alarm rate (CFAR) for  $K$  steps of integration. The overall process of the proposed detection algorithm is described in Algorithm 3.

### B. Constant false alarm rate threshold for detection test

Let us consider the detection threshold  $\mathcal{T}_K$  in (55) for a given constant false alarm rate (CFAR). This threshold can be calculated by using a function of a selected probability of false alarm rate  $P_{fa}$ . For this purpose, we define a likelihood under the noise only signal hypothesis across channels.

We assume that the covariance in the  $m$ th reflection channel is  $\Sigma_m = \sigma_m^2 \mathbf{I}_{LN}$ . We consider the likelihood under the noise only signal hypothesis in the  $m$ th channel by using the sum of received signals in (16). This likelihood is given by

$$l(Z_m | H = H_0) = \mathcal{CN}(\cdot; 0, LN\sigma_m^2), \quad (57)$$

$$\mathbb{E}\{Z_m\} = \mathbb{E}\{Z_{1,m}(r) + \dots + Z_{LN,m}(r)\} = 0$$

$$\mathbb{E}\{Z_m^2\} = \mathbb{E}\{(Z_{1,m}(r) + \dots + Z_{LN,m}(r))^2\} = LN\sigma_m^2,$$

where  $Z_m = \sum_{i=1}^{LN} Z_{i,m}(r)$  denotes the sum of the received signals under the noise only signal hypothesis  $H = H_0$  in

**Algorithm 3** The proposed simultaneous tracking and long time integration algorithm

---

- 1: Initialisation: Generate a set of particles  $\{X_0^p, \zeta_0^p\}_{p=1}^P$
- 2: **for**  $k = 1$  to  $K$  (i.e.,  $K$  CPIs) **do**
- 3:   Collect measurements in  $\mathbf{Z}_k$  given in (16)
- 4:   Prediction: Draw particles
- 5:    $X_k^p \sim p(\cdot | X_{k-1}^p) \quad p = 1, \dots, P$  in (33)
- 6:   Find  $\hat{\Delta t}$  using Algorithm 2
- 7:   Find  $\hat{\alpha}_k$  using Algorithm 1
- 8:   **for**  $p = 1$  to  $P$  **do**
- 9:     Update: Compute  $\tilde{\zeta}_k^p$  together  $\hat{\alpha}_k$  and  $\hat{\Delta t}$  in (35)
- 10:   **end for**
- 11:   Normalise  $\tilde{\zeta}_k^p$  using (34)
- 12:   Degeneracy test in (36)
- 13:   Estimate  $\hat{X}_k$  using (37)
- 14:   Compute the proposed long time integration in (55)
- 15:   Perform the detection test in (56)
- 16: **end for**

---

(16), and,  $\mathbb{E}\{Z_m\}$  and  $\mathbb{E}\{Z_m^2\}$  are the mean and the variance, respectively.

Similarly, the likelihood of the sum of  $M$  channels under the noise only signal hypothesis for  $K$  steps of integration can be evaluated by

$$l(Z_K | H = H_0) = \mathcal{CN}(\cdot; 0, KLN \sum_{m=1}^M \sigma_m^2), \quad (58)$$

where  $Z_K = \sum_{k=1}^K \sum_{m=1}^M Z_{m,k}$  is the sum of  $M$  channels under noise only signal hypothesis for  $K$  steps of integration.

Next, we find the  $P_{fa}$  for the detection test by integrating  $l(Z_K | H = H_0)$  when  $Z_K$  is over the detection threshold  $\mathcal{T}_K$ . Therefore, the  $P_{fa}$  can be defined as

$$\begin{aligned} P_{fa} &= \int_{\mathcal{T}_K}^{+\infty} l(Z_K | H = H_0) dZ_K \\ &= \frac{1}{\pi \sqrt{KLN \sum_{m=1}^M \sigma_m^2}} \int_{\sqrt{KLN \sum_{m=1}^M \sigma_m^2}}^{+\infty} \exp\{-|t|^2\} dt \\ &= \frac{1}{2\sqrt{\pi KLN \sum_{m=1}^M \sigma_m^2}} \text{erfc}\left(\frac{\mathcal{T}_K}{\sqrt{KLN \sum_{m=1}^M \sigma_m^2}}\right), \end{aligned} \quad (59)$$

where  $\text{erfc}(\cdot)$  denotes the complementary error function (see, e.g, [3, Chp.6]). As a result, the threshold  $\mathcal{T}_K$  given  $P_{fa}$  for  $K$  steps of integration using (59) is found as

$$\mathcal{T}_K = \sqrt{KLN \sum_{m=1}^M \sigma_m^2} \text{erfc}^{-1}\left(2\sqrt{\pi KLN \sum_{m=1}^M \sigma_m^2} P_{fa}\right), \quad (60)$$

where  $\text{erfc}^{-1}(\cdot)$  is the inverse complementary error function.

Now, we consider the covariance  $\Sigma_m$  which is satisfied with the following conditions; i) it is a symmetric matrix and ii) is positive semi-definite. In order to find the detection threshold

in this case, we need to perform a linear operation on the measurements which is in the form of a whitening transform with the noise covariance followed by an inner product with the signal model. The measurement likelihood under the noise only signal hypothesis in (16) after the inner product of the measurement and the whitening factor is found as

$$l(\mathbf{W}_m \mathbf{Z}_m(r) | H = H_0) = \mathcal{CN}(\cdot; \mathbf{0}, \mathbf{W}_m^H \Sigma_m \mathbf{W}_m = \mathbf{I}_{LN}) \quad (61)$$

where  $\mathbf{W}_m \in \mathbb{Z}^{LN \times LN}$  is the whitening factor given by  $\mathbf{W}_m = \mathbf{V}_m \mathbf{A}_m^{-\frac{1}{2}}$ , and,  $\mathbf{V}_m$  and  $\mathbf{A}_m$  are the eigenvectors and eigenvalues determined by using the eigenvector-eigenvalue decomposition method of the noise covariance  $\Sigma_m$  in the  $m$ th channel. Afterwards, we easily find the likelihood of the sum of  $M$  channels under the noise only signal hypothesis for  $K$  steps of integration based on the likelihood in (61) thorough (57) and (58), i.e.,

$$l(WZ_K | H = H_0) = \mathcal{CN}(\cdot; 0, KLN M), \quad (62)$$

where  $WZ_K = \sum_{k=1}^K \sum_{m=1}^M W_m Z_{m,k}$  is the sum of  $M$  channels under noise only signal hypothesis for  $K$  steps of integration after applying the whitening factor  $W$ , and  $W_m$  is the whitening factor in the  $m$ th channel. As a result, the corresponding threshold in (60) is found as

$$\mathcal{T}_K = \sqrt{KLN M} \text{erfc}^{-1}\left(2\sqrt{\pi KLN M} P_{fa}\right). \quad (63)$$

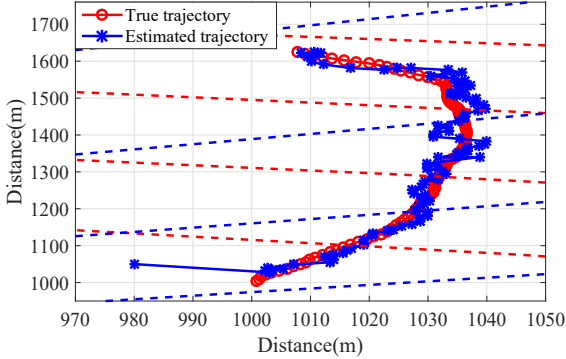
In this section, we have considered the CFAR threshold in both white noise background and non-white noise background. Therefore, given a probability of false alarm rate  $P_{fa}$ , we can calculate  $\mathcal{T}_K$  using (60) when noise background is white. On the other hand, when we have non-white noise background,  $\mathcal{T}_K$  can be determined by using (63) for the likelihood ratio test in for  $K$  steps of integration. Now, we use this CFAR threshold for the detection test in (55).

## VI. EXAMPLE

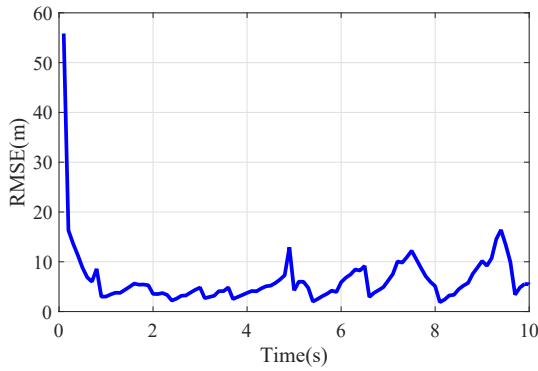
In this section, we demonstrate the proposed algorithm through an example and compare the efficacy of this approach with conventional techniques. We consider a scenario in which a ULA receiver co-located with a transmitter is at the origin of the 2D Cartesian plane, and, a separated transmitter is located at [10m, 500m] (see. Fig.. 2). In this setting,  $M = 2$  transmitters emit  $N = 20$  linear frequency modulated (i.e.,

TABLE I  
TRANSMITTED SIGNAL PARAMETERS

Parameter	Value
Carrier frequency $f_c$	10GHz
Bandwidth $B$	1MHz
Pulse repetition interval (PRI) $T$	100us
Coherent processing interval (CPI) $\Delta$	0.1s
Number of pulses during a CPI $N$	20
Number of elements in ULA $L$	20
Number of transmitters $M$	2



(a) Typical scenario for an estimated trajectory



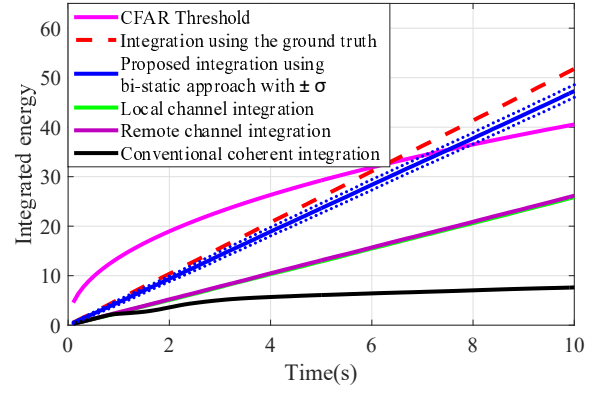
(b) Root mean square error (RMSE)

Fig. 5. Example scenario: (a) A low SNR (-6dB) object moves the true trajectory (red line) across range (red dashed lines) and bearing (blue dashed lines) bins. The proposed algorithm estimates the object trajectory (blue line) for detection test. (b) RMSE (blue line) of this trajectory estimate obtained in (a).

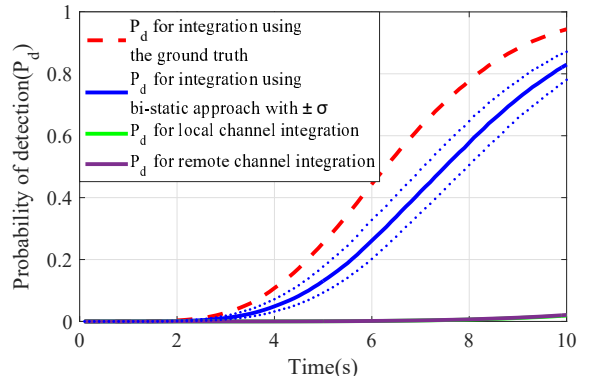
up-chirp) waveforms in a CPI towards a surveillance region. In this region, there is a low SNR object with an initial state  $X_0 = [1000\text{m}, 1000\text{m}, 10\text{m/s}, 50\text{m/s}]$  moving along an unknown trajectory according to the object dynamic model defined in (25). The ULA receiver collects measurements in accordance with the signal model in (16) in the local and the remote channels as well as the direct channel.

The parameters of the transmitted pulses used in this example are shown in Table I. Given these parameters, we calculate the bearing resolution as  $\Delta\theta = 5.1^\circ$  given by  $\Delta\theta = \sin^{-1}(\frac{0.8192}{L})$ , and, the range resolution as  $\Delta\tau = 150\text{m}$  given by  $\Delta\tau = \frac{c}{2B}$  (see, e.g., [22]). Fig. 5 illustrates these corresponding resolutions, where the blue dashed and the red dashed lines indicate the bearing and the range resolutions, respectively. We also find the velocity resolution as  $\Delta V = 7.5\text{m/s}$  by using  $\Delta V = \frac{\lambda_c}{2NT}$  (or, equivalently, the Doppler resolution  $\Delta\omega = 4\pi f_c \frac{\Delta V}{c} T$  as  $0.314\text{deg/s}$ ).

We use the proposed algorithm to test the object existence hypothesis in the receiver's resolution bins with  $P = 400$  particles. These particles are initially selected as a  $20 \times 20$  element uniform grid within the bin under test. We perform long time integration using (55) spanning 10s with a CPI interval of 0.1s. The complex reflection coefficient for each channel is also generated using a complex Gaussian density leading to an expected SNR of  $-6\text{dB}$ . For synchronisation, we deal with the synchronisation term  $\Delta t$  in the remote channel as an unknown time shift and randomly select  $\Delta t$  in the range



(a) Long-time integration



(b) Probability of detection

Fig. 6. Long-time integration: (a) The average proposed integration (blue line) using the proposed algorithm versus the integration with ground truth (red dashed line) compared to the detection (CFAR) threshold (magenta line). The conventional coherent (black line), the local channel (green line), and the remote channel (purple line) integration fail to exceed the detection threshold. (b) The corresponding probabilities of detection ( $P_d$ ) with the same colour code found in (a).

of  $0 < \Delta t < PRI$  so that each received pulse in the remote channel contains the unknown time shift. We also generate the direct signals with additive noise using (51) leading to an expected SNR of  $0\text{dB}$ .

In this example, when an object is located in the bin under test, the particles generated by the proposed algorithm converge to the underlying state of the object, and, the integrated value using the proposed integration in (55) increases. When this value is over the detection threshold, the proposed algorithm selects the object existence hypothesis. On the other hand, when the bin under test contains no object, the particles start to diverge in space due to very small and similar likelihood values. Fig. 5(a) illustrates a typical trajectory estimate using the proposed algorithm, which indicates that the trajectory estimate (blue line) is reasonably close to the true trajectory (red line). Fig. 5(b) shows the root mean square error (RMSE) of this trajectory estimate (blue line) obtained in Fig. 5(a), where the RMSE provides a reasonably low value after only a few steps (i.e., each step represents a CPI).

Now, we consider long time integration. For this purpose, we generate 100 measurement sets using (16) with unknown object trajectories described in Fig. 5.

Fig. 6(a) illustrates the average integrated value (blue solid line) with  $\pm 1$  standard deviation bounds (blue dotted line)

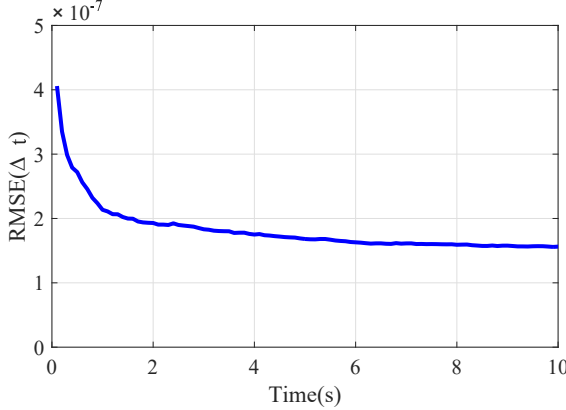


Fig. 7. RMSE of the synchronised term estimated by using the bi-static synchronisation approach (blue solid line) and using the multi-static synchronisation approach (orange solid line)

using the proposed integration in (55). It can be seen that the integrated value using the proposed integration increases up to 47.9 at  $t = 10$ s, which is relatively close to the best achievable value (red dashed line) 51.78 using the full knowledge of the ground truth values of the true trajectory and the synchronisation term of the remote channel.

For object detection, we calculate the detection threshold as the CFAR threshold (magenta line) using (60) for the given probability of false alarm rate  $P_{fa} = 10^{-8}$  and compare the integrated values against this threshold. It is clearly observed that the integrated value using the proposed approach exceeds the CFAR threshold at  $t = 7.1$ s, while both the local channel (green solid line) and the remote channel (purple solid line) integration stay under the noise only signal hypothesis. The conventional coherent integration (black solid line) also selects the noise only signal hypothesis. Note that, when the integration is used with an individual channel, this integrated value fails to exceed the detection threshold due to the inferior tracking performance.

Now, we consider the probability of detection  $P_d$  as the function of the integrated value over time, and, calculate this probability for the proposed algorithm empirically. Fig. 6(b) illustrates the  $P_d$  (blue solid line) with  $\pm 1$  standard deviation bounds (blue dotted lines) for the proposed integration compared to the  $P_d$  (red dashed line) obtained by the best achievable integration. It is clearly shown that the  $P_d$  using the proposed integration increases over time and reaches 0.84 at  $t = 10$ s, whereas both  $P_d$ s for the local (green solid line) and the remote integration (purple solid line) reach almost zero and fail to detect the object in an overwhelming majority of the experiences.

Next, we evaluate estimation of the unknown time shift  $\Delta t$  as the synchronisation term in the remote channel. For this purpose, we calculate the RMSE of the estimated  $\Delta t$  by using

$$RMSE(\Delta t_k) = \sqrt{\frac{\sum_{l=1}^{L_s} (\Delta \hat{t}_{l,k} - \Delta t)^2}{L_s}}, \quad (64)$$

where  $\Delta t$  indicates the true synchronisation term,  $\Delta \hat{t}_{l,k}$  is the  $l$ th estimate of  $\Delta t$  at the  $k$ th CPI and  $L_s = 100$  is the total number of the measurements.

Fig. 7 illustrates the RMSE of  $\Delta t$  estimated by using Al-

gorithm 2. It is clearly recognised that the RMSE of  $\Delta t$  (blue line) has lower value over time and is  $1.5e-7$  at  $t = 10$ s.

The benefits of this proposed approach come with some additive cost of computations compared to conventional integration methods. The computational cost of the bin under test for detection using the proposed algorithm at the  $k$ th CPI requires  $P(N_X^2 + 2N_{I_1}N_{I_2}M(LN)^2)$  multiplications and  $P(1 + 2N_{I_1}N_{I_2}M(LN - 1))$  additions, while conventional coherent integration requires  $M$  multiplications and  $M(LN - 1)$  additions. Here,  $P$  is the total number of particles,  $N_X$  denotes the dimensionality of the object state in (25), and,  $N_{I_1}$  and  $N_{I_2}$  are the number of iterations for the EM algorithm in Algorithm 1 and the golden selection search in Algorithm 2, respectively.

## VII. CONCLUSION

In this work, we have proposed the detection approach, which can perform simultaneous trajectory estimation and log time integration for detecting a manoeuvring and low SNR object in mono-static, bi-static, and multi-static configurations. We demonstrate that the proposed algorithm enables us to collect the entire evidence of object existence at the receiver by i) coherently integrating both mono-static and bi-static channels within a CPI, ii) performing non-coherent integration across different channels, and, iii) continuing integration for an arbitrarily long interval that contains many CPIs. As a result, the proposed integrated value is close to the best achievable integrated value using the ground truth values of the true trajectory and the synchronisation term of the remote channel. This approach also enables us to detect manoeuvring and low SNR objects which cannot be detected using other techniques. Future work includes further experimentation for the characterisation of this detection approach under different SNR working conditions.

## APPENDIX A LIKELIHOOD LOCALITY

Let us consider the likelihood ratio test in (18) with the locality of the measurements  $\mathbf{Z}_{m,k}(r) \in \mathcal{E}_m(X_k)$  to  $X_k$ . Let us define the complement of  $\mathcal{E}$  in the set of range bins, i.e.,  $\bar{\mathcal{E}} \triangleq \{1, 2, \dots, \Gamma\} \setminus \mathcal{E}_m(X_k)$ . It can easily be seen that

$$\begin{aligned} l(\mathbf{Z}_{m,k}|X_k, \alpha_{m,k}, \Delta t_m, H = H_1) = \\ \prod_{r \in \mathcal{E}_m} l(\mathbf{Z}_{m,k}(r)|X_k, \alpha_{m,k}, \Delta t_m, H = H_1) \prod_{r' \in \bar{\mathcal{E}}_m} p(\mathbf{Z}_{m,k}(r')). \end{aligned} \quad (65)$$

Similarly, the likelihood for the noise-only signal hypothesis factorises as

$$\begin{aligned} l(\mathbf{Z}_{m,k}|X_k, H = H_0) = \\ \prod_{r \in \mathcal{E}_m} l(\mathbf{Z}_{m,k}(r)|H = H_0) \prod_{r' \in \bar{\mathcal{E}}_m} p(\mathbf{Z}_{m,k}(r')), \end{aligned} \quad (66)$$

which, after substituting into (18) with (65) leads to (21).

## APPENDIX B

### THE FISHER INFORMATION MATRIX FOR THE ML REFLECTIVITY ESTIMATOR

We give derivation of a Fisher information matrix of the reflection coefficients. In general, a Fisher matrix is found by taking the second order partial derivative of a log-likelihood with respect to unknown parameters of the likelihood [29, Chp.3]. In our problem setting, we find the Fisher matrix of the reflection coefficients by taking the second order partial derivative of the log-likelihood in (45) with respect to the reflection coefficients with the full knowledge of the object kinematic  $X$  and the synchronisation term, i.e.,

$$\begin{aligned} \mathbf{I}(\boldsymbol{\alpha}) &= \begin{bmatrix} -\mathbb{E}\left\{\frac{\partial^2 \log l(\mathbf{Z}|\boldsymbol{\alpha})}{\partial \alpha_1^2}\right\} & \dots & -\mathbb{E}\left\{\frac{\partial^2 \log l(\mathbf{Z}|\boldsymbol{\alpha})}{\partial \alpha_1 \partial \alpha_M}\right\} \\ \vdots & \ddots & \vdots \\ -\mathbb{E}\left\{\frac{\partial^2 \log l(\mathbf{Z}|\boldsymbol{\alpha})}{\partial \alpha_M \partial \alpha_1}\right\} & \dots & -\mathbb{E}\left\{\frac{\partial^2 \partial^2 \log l(\mathbf{Z}|\boldsymbol{\alpha})}{\partial \alpha_M^2}\right\} \\ \sum_{r \in \mathcal{E}_1(X)} 2\tilde{s}_1(r, X) & \dots & 0 \\ \vdots & \ddots & \vdots \\ 0 & \dots & \sum_{r \in \mathcal{E}_M(X)} 2\tilde{s}_M(r, X) \end{bmatrix} \end{aligned} \quad (67)$$

where  $\mathbf{I}(\boldsymbol{\alpha}) \in \mathbb{C}^{M \times M}$  is the diagonal matrix, which has the diagonal elements as a variance of each reflection coefficient, and  $\tilde{s}_m(r, X) \triangleq \mathbf{s}_m(r, X)^H \Sigma_m^{-1} \mathbf{s}_m(r, X)$  in the  $m$ th channel.

## REFERENCES

- [1] M. Richards, W. Melvin, J. Scheer, J. Scheer, and W. Holm, *Principles of Modern Radar: Radar Applications*, ser. Electromagnetics and Radar. Institution of Engineering and Technology, 2014.
- [2] S. Haykin, "Cognitive radar: a way of the future," *IEEE Signal Processing Magazine*, vol. 23, no. 1, pp. 30–40, Jan 2006.
- [3] M. Richards, *Fundamentals of Radar Signal Processing*, ser. Professional Engineering. McGraw-hill, 2005.
- [4] X. Chen, J. Guan, N. Liu, and Y. He, "Maneuvering target detection via radon-fractional fourier transform-based long-time coherent integration," *Signal Processing, IEEE Transactions on*, vol. 62, no. 4, pp. 939–953, Feb 2014.
- [5] L. Kong, X. Li, G. Cui, W. Yi, and Y. Yang, "Coherent integration algorithm for a maneuvering target with high-order range migration," *IEEE Transactions on Signal Processing*, vol. 63, no. 17, pp. 4474–4486, Sept 2015.
- [6] Y. Boers and J. Driessens, "Multitarget particle filter track before detect application," *Radar, Sonar and Navigation, IEE Proceedings*, vol. 151, no. 6, pp. 351–357, Dec 2004.
- [7] E. Grossi, M. Lops, and L. Venturino, "A novel dynamic programming algorithm for track-before-detect in radar systems," *Signal Processing, IEEE Transactions on*, vol. 61, no. 10, pp. 2608–2619, May 2013.
- [8] H. L. Van Trees, *Detection, Estimation, and Modulation Theory: Radar-Sonar Signal Processing and Gaussian Signals in Noise*. Melbourne, FL, USA: Krieger Publishing Co., Inc., 1992.
- [9] S. Davey, M. Rutten, and B. Cheung, "Using phase to improve track-before-detect," *Aerospace and Electronic Systems, IEEE Transactions on*, vol. 48, no. 1, pp. 832–849, Jan 2012.
- [10] M. Unay, B. Mulgrew, and D. Clark, "Maximum likelihood signal parameter estimation via track before detect," pp. 1–5, Sept 2015.
- [11] O. Rabaste, C. Riche, and A. Lepoutre, "Long-time coherent integration for low SNR target via particle filter in track-before-detect," in *Information Fusion (FUSION), 2012 15th International Conference on*, July 2012, pp. 127–134.
- [12] K. Kim, M. Unay, and B. Mulgrew, "Detection of manoeuvring low SNR objects in receiver arrays," in *2016 Sensor Signal Processing for Defence (SSPD)*, Sept 2016, pp. 1–5.
- [13] ———, "Simultaneous tracking and long time integration for detection in collaborative array radars," in *2017 IEEE Radar Conference (Radar-Conf)*, May 2017, pp. 0200–0205.
- [14] H. Godrich, A. Haimovich, and R. Blum, "Target localization accuracy gain in MIMO radar-based systems," *Information Theory, IEEE Transactions on*, vol. 56, no. 6, pp. 2783–2803, June 2010.
- [15] R. Niu, R. Blum, P. Varshney, and A. Drozd, "Target localization and tracking in noncoherent multiple-input multiple-output radar systems," *Aerospace and Electronic Systems, IEEE Transactions on*, vol. 48, no. 2, pp. 1466–1489, April 2012.
- [16] T. K. Moon, "The Expectation-Maximization Algorithm," *IEEE Signal Processing Magazine*, vol. 13, no. 6, pp. 47–60, Nov 1996.
- [17] B. Carlin and T. Louis, *Bayes and Empirical Bayes Methods for Data Analysis, Second Edition*, ser. Chapman & Hall/CRC Texts in Statistical Science. Taylor & Francis, 2010.
- [18] A. Haimovich, R. Blum, and L. Cimini, "MIMO radar with widely separated antennas," *Signal Processing Magazine, IEEE*, vol. 25, no. 1, pp. 116–129, 2008.
- [19] J. Li and P. Stoica, *MIMO Radar Signal Processing*. John Wiley & Sons, Inc., Hoboken, NJ, 2009.
- [20] A. De Maio and M. Lops, "Design principles of MIMO radar detectors," *Aerospace and Electronic Systems, IEEE Transactions on*, vol. 43, no. 3, pp. 886–898, July 2007.
- [21] Y. Yang and R. S. Blum, "MIMO radar waveform design based on mutual information and minimum mean-square error estimation," *IEEE Transactions on Aerospace and Electronic Systems*, vol. 43, no. 1, pp. 330–343, January 2007.
- [22] H. L. Van Trees, *Optimum Array Processing*. New York: Wiley-Interscience, 2002.
- [23] S. Kay, *Fundamentals of Statistical Signal Processing: Detection theory*, ser. Prentice Hall Signal Processing Series. Prentice-Hall PTR, 1998.
- [24] S. A. B. Ristic and N. Gordon, *Beyond the Kalman Filter: Particle Filters for Tracking Applications*. Artech House, 2004.
- [25] K. Murphy, *Machine Learning: A Probabilistic Perspective*, ser. Adaptive computation and machine learning. MIT Press.
- [26] M. Orton and W. Fitzgerald, "A Bayesian approach to tracking multiple targets using sensor arrays and particle filters," *Signal Processing, IEEE Transactions on*, vol. 50, no. 2, pp. 216–223, Feb 2002.
- [27] M. Arulampalam, S. Maskell, N. Gordon, and T. Clapp, "A tutorial on particle filters for online nonlinear/non-gaussian bayesian tracking," *Signal Processing, IEEE Transactions on*, vol. 50, no. 2, pp. 174–188, Feb 2002.
- [28] W. H. Press, S. A. Teukolsky, W. T. Vetterling, and B. P. Flannery, *Numerical Recipes in C (2Nd Ed.): The Art of Scientific Computing*. New York, NY, USA: Cambridge University Press, 1992.
- [29] S. M. Kay, *Fundamentals of Statistical Signal Processing: Estimation Theory*. Upper Saddle River, NJ, USA: Prentice-Hall, Inc., 1993.